Minimal attachment of Pseudomonas aeruginosa to DNA modified surfaces

Hitesh Pingle, Peng-Yuan Wang, Rosalia Cavaliere, Cynthia B. Whitchurch, Helmut Thissen, and Peter Kingshott

Citation: Biointerphases **13**, 06E405 (2018); doi: 10.1116/1.5047453
View online: https://doi.org/10.1116/1.5047453
View Table of Contents: http://avs.scitation.org/toc/bip/13/6
Published by the American Vacuum Society

Minimal attachment of *Pseudomonas aeruginosa* to DNA modified surfaces

Hitesh Pingle,[1] Peng-Yuan Wang,[1,a)] Rosalia Cavaliere,[2] Cynthia B. Whitchurch,[2] Helmut Thissen,[3] and Peter Kingshott[1,a)]
[1]*Department of Chemistry and Biotechnology, Swinburne University of Technology, Hawthorn, Victoria, Australia*
[2]*The ithree institute, University of Technology Sydney, Ultimo, New South Wales 2007, Australia*
[3]*CSIRO Manufacturing, Clayton, Victoria, Australia*

(Received 6 July 2018; accepted 26 September 2018; published 16 October 2018)

Extracellular deoxyribonucleic acid (eDNA) exists in biological environments such as those around medical implants since prokaryotic or eukaryotic cells can undergo processes such as autolysis, necrosis, and apoptosis. For bacteria, eDNA has been shown to be involved in biofilm formation and gene transfer and acts as a nutrient source. In terms of biofilm formation, eDNA in solution has been shown to be very important in increasing attachment; however, very little is known about the role played by surface immobilized eDNA in initiating bacterial attachment and whether the nature of a DNA layer (physically adsorbed or covalently attached, and molecular weight) influences biofilm formation. In this study, the authors shed light on the role that surface attached DNA plays in the early biofilm formation by using Si wafers (Si) and allylamine plasma polymer (AAMpp) coated Si wafers to adsorb and covalently immobilize salmon sperm DNA of three different molecular weights. *Pseudomonas aeruginosa* was chosen to study the bacterial interactions with these DNA functionalized surfaces. Characterization of surface chemistry and imaging of attached bacteria were performed via x-ray photoelectron spectroscopy (XPS), scanning electron microscopy, and epi-fluorescence microscopy. XPS results confirmed the successful grafting of DNA on the AAMpp and Si surfaces, and surprisingly the results showed that the surface attached DNA actually reduced initial bacterial attachment, which was contrary to the initial hypothesis. This adds speculation about the specific role played by DNA in the dynamics of how it influences biofilm formation, with the possibility that it could actually be used to make bacterial resistant surfaces. *Published by the AVS.* https://doi.org/10.1116/1.5047453

I. INTRODUCTION

Extracellular deoxyribonucleic acid (eDNA) is the most abundant biopolymer present in both aquatic and terrestrial environments with a concentration level of up to 2 μg/g in the uppermost layer of soil, while it can reach almost 0.5 g/m^2 in the top centimeter of deep sea deposits.[1–3] Researchers have shown that eDNA plays a significant role in bacterial life cycles including biofilm formation in both Gram negative and Gram positive bacteria.[4,5] The dynamic role of eDNA in biofilm formation was demonstrated by Whitchurch *et al.*,[6] who treated *Pseudomonas aeruginosa* biofilms with DNase. They found that the enzyme could remove eDNA and help dissolve the biofilm. Conover *et al.*[7] also showed the importance of eDNA in the maintenance of *Bordetella bronchiseptica* biofilms, where they used DNase I to degrade a biofilm of *B. bronchiseptica* in a mouse respiratory tract. Since then, the active role of eDNA in the ability of different microbes to form biofilms has been studied. Most of the studies showed that individual bacteria can release eDNA or it can come from cell lysis. Bacteria can use eDNA as a nutrient source, for repairing their own DNA, and it can be used as a building block in bacterial biofilms.[3] Research by Das *et al.*[8] showed that the presence of eDNA on *Streptococcus mutans* cell surfaces increased adhesion strength on both hydrophilic and hydrophobic surfaces. Furthermore, most of the studies have investigated what role suspended DNA or DNA released by bacteria play in biofilm formation and stability, including how it initiates bacterial attachment to surfaces. However, very little work has been devoted to precisely understanding the role that pre-adsorbed DNA on surfaces has in initial bacterial attachment and subsequently how the adsorbed/immobilized DNA can influence biofilm formation. This is important because it raises the question whether DNA can actually adsorb to surfaces from suspension and enhance attachment or it may be the case that it is only needed in the environment above the substrate surface to enhance colonization and biofilm development.

This study was aimed at determining whether a surface layer of DNA can influence bacterial attachment and whether the stability (achieved by covalent attachment) is an important property of the DNA layer. We utilized a model DNA from salmon sperm since it can easily be manipulated in terms of size and it is likely to have a similar average composition to eDNA. We use plasma polymerization of allylamine to generate a reactive, amine rich surface on Si wafer substrates for covalent immobilization of DNA that was compared to physical adsorption. An advantage of plasma polymerization is the generation of mechanically stable thin

a)Authors to whom correspondence should be addressed: pkingshott@swin.edu.au and pengyuanwang@swin.edu.au

films with similar chemistry to that of the starting monomer.[9] An additional variable to the study was investigating the role of DNA molecular weight on bacterial attachment. In this case, we used three differently sized DNA including <500 bp DNA, ~5–15 kbp DNA, and >20 kbp that were made by sonication of the starting salmon sperm DNA salt. Covalent immobilization of the different DNAs on allylamine plasma polymer (AAMpp) surfaces was achieved using carbodiimide chemistry,[10,11] and both the physically adsorbed and covalently immobilized DNA surfaces were tested against *Pseudomonas aeruginosa* attachment.

II. EXPERIMENT

A. Materials

Boron doped silicon wafers with a nominal oxide layer of 2 nm, diameter 100 mm, orientation (100), and a resistivity 1–10 Ω cm were obtained from M.M.R.C. Pty Ltd. (Malvern, Australia). Flat bottom tissue culture polystyrene (TCPS) multiwell plates (12 and 6 wells) were purchased from Sarstedt Australia Pty Ltd.

Absolute ethanol (AR grade), Milli-Q water, and allylamine were purchased from Chem Supply Australia. Sodium phosphate (Na_3PO_4), phosphate buffered saline (PBS), sodium hydroxide, DNA sodium salt from salmon testes (DNA) (Catalog no. D1626), and the carbodiimide chemistry reagents, *N*-(3-dimethylaminopropyl)-*N*′-ethylcarbodiimide hydrochloride (EDC), *N*-hydroxysuccinimide (NHS), and ethylenediamine tetraacetic acid (EDTA), were purchased from Sigma-Aldrich, Australia. 1.5% w/v tryptic soy agar, tryptic soy broth, and Luria broth agar (LBA) for bacterial culture were purchased from Thermo Fisher Scientific. Müller-Hinton agar and Müller-Hinton broth (MHB) were purchased from BD (Becton Dickinson). Live/Dead BacLight, bacterial viability kits [3.34 mM propidium iodide (PI) in dimethyl sulfoxide (DMSO) and 20 mM of SYTO 9 in DMSO] were purchased from Invitrogen Life Technologies. 4,6-diamidino-2-phenylindole (cat#D9542) dye was purchased from Sigma-Aldrich, USA. The *P. aeruginosa* strain PAO1 (ATCC 15692) used in this study was purchased from American Type Culture Collection.

B. Plasma polymerization

Radio-frequency glow discharge (rfgd) plasma polymerization was accomplished in a custom-built reactor as described previously.[12] In short, the height of a cylindrical reactor chamber was 350 mm with a diameter of 170 mm. The distance between the top and bottom circular electrode was 150 mm. Allylamine monomer was used to generate thin films of AAMpp. In the next step, silicon wafers were cut into a size of $1.5 \times 1.5\ cm^2$ and cleaned by 15 min sonication in ethanol followed by drying with N_2 gas. Si substrates were then treated with a UV-ozone cleaner (BioForce Nanoscience, IA, USA) for 30 min to achieve a more hydrophilic surface. The cleaned Si wafers were placed on the lower rectangular/circular electrode for AAMpp deposition. Prior to plasma coating, the monomer was degassed and refilled into the chamber three times. Polymerization parameters chosen for deposition of the AAMpp coating were a treatment time of 25 s, an initial monomer pressure of 0.2 mbar, and a load power of 20 W. During plasma deposition, the pressure increased slightly to 0.25 mbar.

C. Different size DNA preparation and size characterization

Three differently sized (short to long) DNAs were prepared by sonication for different lengths of time. In brief, 4 mg/ml of salmon sperm DNA was dissolved in 7 ml of Milli-Q water at 37 °C on a rotating wheel. The following day, the DNA was sonicated for various numbers of 2 min cycles on ice such that for a DNA size <500 bp a 5 × 2 min cycle was used; for a DNA size between 5 and 15 Kbp a 2 × 2 min cycle was used, and for a DNA size >20 Kbp DNA the solution was not sonicated.

DNA samples were size separated by electrophoresis through a 1% (w/v) agarose gel (Fig. 1) and stained with Gel Red (Biotium). The sizes of DNA samples were estimated by referencing to a standard DNA ladder (1 Kb DNA ladder; New England BioLabs; size range: 500 bp to 10 kb). DNA was visualized with the InGenius 3 Gel Documentation System (Syngene) or the EDAS 290 Electrophoresis Documentation and Analysis System (Kodak). The images were acquired with the GeneSys software v1.5.0.0 or the KODAK MOLECULAR IMAGING software v5 for the respective devices.

D. DNA functonalization, adsorption, and covalent attachment on substrates

Salmon sperm DNA solutions (2 mg/ml) of the three different sizes of DNA were prepared in PBS with EDTA:

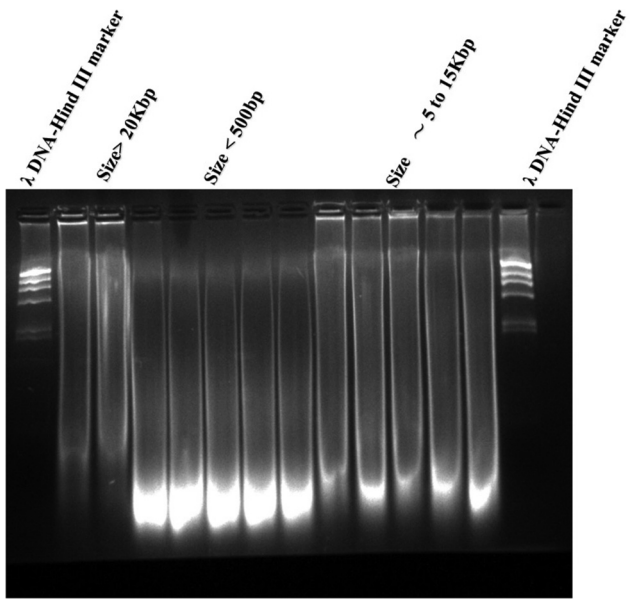

FIG. 1. Agarose gel electrophoresis of different sized salmon sperm DNA used in this study. λ DNA- Hind III marker (lane and right corner); unsonicated salmon sperm DNA >20 kbp (left); sonicated salmon sperm DNA ~5–15 kbp (right); sonicated salmon sperm DNA <500 bp (middle).

10 mM sodium phosphate, 0.15 M NaCl, 10 mM EDTA, *p*H 7.2. Physical adsorption from DNA solutions was performed on Si wafers and AAMpp surfaces. 2000 μl of each DNA solution was drop casted onto a $1 \times 1\,cm^2$ area of each surface, kept in 12 well TCPS plates and incubated overnight at room temperature. Covalent attachment of DNA was performed on AAMpp surfaces through mixing 125 mM EDC and 125 mM NHS and DNA in PBS. In the next step, the solution was drop-cast onto AAMpp surfaces and incubated overnight at room temperature. After incubation, all surfaces were washed three times with sterile Milli-Q water for further studies. A thick film of DNA was also prepared by repeated pipetting of a DNA solution (up to eight times) onto polystyrene slides in order to determine the bulk elemental composition of DNA.

E. X-ray photoelectron spectroscopy

X-ray photoelectron spectroscopy (XPS) analysis was performed using a Kratos AXIS NOVA spectrometer (Kratos Analytical Inc., Manchester, UK) with a monochromated $Al_{k\alpha}$ x-ray source operating at a power of 150 W. Survey and high resolution spectra were acquired at 160 and 20 eV pass energies, respectively. Three spots on each surface, with three replicates, with an elliptical area of approximately $0.3 \times 0.7\,mm^2$ were analyzed. Atomic concentrations of detected elements were calculated via integral peak intensities and the sensitivity factors provided by the instrument manufacturer. However, for effective charge compensation, standard operating conditions were filament current 1.8 Å, charge balance 3.3 V, and bias voltage 1.3 V. Obtained data analysis and quantification were performed using CASAXPS processing software version 2.3.16 (Casa Software Ltd., Teignmouth, UK). A linear background was chosen for quantification. Gaussian broadened Lorentzian line shape [GL(30)] was used for high resolution curve fits. All the spectra were charge corrected to the CHx component at 285.0 eV. Peaks were restricted to full width half maximum between 1 and 1.9 eV.

F. Thickness of DNA films

To calculate the thickness and surface coverage of adsorbed/immobilized DNA on Si and AAMpp surfaces, the XPS data were used. Based on some assumptions, the thickness (Z) of adsorbed/immobilized DNA (in the dry state) was calculated using the overlayer equation shown below

$$Z = -\lambda_{IMFP} \times \cos\theta \times \ln\left(1 - \frac{I}{I_\infty}\right),$$

where I and I_∞ are the %N or %P recorded on the DNA coated surfaces and the %N or %P for bulk DNA, respectively. λ_{IMFP} is the mean free path of N 1s (3.3 nm) or P 2p (3.9 nm) photoelectrons generated from the DNA overlayers calculated according to the literature[13,14] and θ is the angle between the analyzer and the sample, which was 0° for all flat Si/AAMpp surfaces. The reference value for I_∞ was determined by two different manual calculations. The first calculation for the %N or %P for bulk DNA is based on the given Sigma-Aldrich (catalog no. D1626) composition of the base pair content [i.e., guanine-cytosine (GC): 41.2%, adenine-thymine (AT): 58.8%]. The second calculation is based on the assumption that DNA has equal base pairs (AT: GC). According to the first calculation, the values of I_∞ for N and P were determined to be 11.06% and 5.96%, respectively, and based on the second assumption, i.e., equal base pairs in DNA, the values of I_∞ for N and P were determined to be 17.4% and 4.65%, respectively.

Once the thickness of each DNA modified surface was determined, the surface coverage was calculated in ng/cm^2 assuming the density of dry DNA was 1.7 g/cm^3.[15–17] This calculation was based on the assumption that the surface was uniformly covered with DNA, capturing a volume of 1 cm × 1 cm × Z.

$$\Theta = Z \times 1.7 \times 10^2.$$

To calculate thickness and surface coverage of DNA on Si surfaces, the N 1s signal of DNA was used because the P 2p signal from DNA overlaps with the Si plasmon bands. For DNA surface coverage determination on the AAMpp surfaces, the P 2p signal was used since the N 1s signal for the control AAMpp is too high to see any significant differences.

G. *P. aeruginosa* culture and attachment assays

After successful adsorption and covalent attachment of DNA on the different surfaces, surfaces were used for static bacterial culture. 1.5% LBA plate was inoculated with *P. aeruginosa* strain PAO1 (ATCC 15692) thawed from −80 °C stock. The plate was incubated for 18 h at 37 °C. A single colony was transferred from the agar plate into 2 ml of MHB in an Eppendorf tube for overnight (O/N) culture at 37 °C. 1 ml of the O/N culture was removed, and the bacteria were washed three times with 1 ml fresh MHB. The bacteria were resuspended in 1 ml MHB and diluted 1/100 of the overnight culture density in 2 ml of MHB and cultured for 2 h at 37 °C with shaking. After 2 h, the bacteria were diluted 1/100 in MHB media. These steps are included to remove eDNA from overnight culture and to allow the bacteria to enter exponential growth prior to commencing the biofilm attachment assay. The next step involved diluting the bacterial MHB media which was added on top of the physically adsorbed and covalently immobilized DNA surfaces including the Si control, facing up, in 12 well TCPS plates for static culture at 37 °C for different time points. After completion of the incubation time, surfaces were rinsed three times with PBS buffer, to remove the nonattached bacteria.

H. Live/dead staining of bacteria

In order to investigate the initial bacterial attachment on Si and plasma coated surfaces in a quantitative manner, the

rinsed samples of attached bacteria were first fixed using 2 ml of 3.7% (v/v) formaldehyde in Milli-Q water. In the following step, surfaces were rinsed three times with PBS buffer and finally the bacteria staining with the Live/Dead (SYTO 9/PI) dye, which is a two-color fluorescence dye of bacterial viability. After staining with fluorescence dye, when excited at 480–490 nm, bacteria emit green fluorescence (500 nm, emission wavelength) when alive or red fluorescence (635 nm, emission wavelength) when dead. However, as described above we have fixed bacteria using formaldehyde treatment, so using this fluorescence dye we have obtained only red fluorescence images of static culture (37 °C) sample surfaces. The Live/Dead staining solution was prepared according to the standard operating protocols. 2 ml of the Live/Dead dye solution was added on each sample surface for 30 min in the dark followed by rinsing with PBS for 5 min.

All fluorescent images were captured using an inverted Epi-fluorescence microscopy with 20× lens (Eclipse Ti-Nikon, Instruments Inc., Japan). The experiment was performed in duplicate. The area covered by PI stained bacteria of each image was analyzed using NIH IMAGEJ 1.48v software. The percentage surface area occupied by bacteria was calculated by thresholding the images until only the bacterial cells were detected in the IMAGEJ 1.48v software and then measuring the total area. For statistical analysis, ten images (20×: 449.35 μm^2) from two surfaces of each sample were analyzed ($n = 10$) with the help of one-way ANOVA software.

I. Scanning electron microscopy

Scanning electron microscopy (SEM) was also used to image the attached bacteria that were first fixed using 3.7% (v/v) formaldehyde as described in Sec. II H. These samples were rinsed with Milli-Q water and dried at room temperature. Prior to imaging, all samples were sputter coated with approximately 15 nm Au. Samples were analyzed using ZEISS SUPRA 40 SEM (VP Carl Zeiss SMT, Germany) at 3–5 keV.

III. RESULTS AND DISCUSSION

A. XPS analysis of physically and covalently immobilized DNA

XPS analysis was performed on the different surfaces to determine the elemental composition and success of the modification steps. Samples included DNA absorbed Si surfaces, DNA physically (PDNA) and covalently (CDNA) immobilized to the AAMpp surfaces, and the Si, AAMpp, and bulk DNA controls.

The results from the XPS analysis are shown in Table I and include the elemental composition and atomic ratios of bulk DNA, the control Si/AAMpp surfaces, and all DNA functionalized surfaces. Bulk DNA showed the presence of O (30.3%), C (48.3%), N (8.8%), P (3.5%), and Na (7.7%) as was expected.[18–20] Thereafter, these data were used as confirmation of DNA immobilization on the different surfaces (Si wafers and AAMpp). Analysis of the untreated Si wafer control showed the presence of Si (55%), O (35%), and low levels C (9.9%) from adventitious hydrocarbon contamination. The high Si content indicates that the SiO_2 layer is thinner than the XPS sampling depth of 10 nm.

Confirmation of the successful physical adsorption of DNA (PDNA) to the Si wafer surfaces was the fact there was a decrease in Si signal, a subsequent increase in C content, and also the presence of N for the three differently sized DNA (500 bp, 5–15 kbp, and 20 kbp) molecules. The decrease in the O/C ratio was expected from the composition of DNA. Similar levels of the larger DNA (5–15 and 20 kbp) adsorb to the Si wafers compared to the smallest DNA (500 bp), where less N was detected. Also, due to the overlap in peak position between the Si plasmon peaks and the P peaks it was not possible to determine the P content arising from adsorbed DNA.

In order to provide more chemical information about the different DNA coated surfaces, high resolution analysis was performed followed by curve-fitting to assign chemical functionalities. The C 1s spectrum for the control Si wafer surface is shown in Fig. 2(a). Four components were

TABLE I. XPS elemental composition and atomic ratios (O/C and N/C) of the control Si and AAMpp surfaces and those coated with differently sized DNA (<500 bp, ~5–15 kbp, >20 kbp), both physically adsorbed (PDNA) and covalently immobilized (CDNA). Shown are mean values ± standard deviation based on three analyses performed on each type of sample ($n = 3$).

Sample	%Si	%O	%N	%C	%P	%Na	Traces of Cl	O/C	N/C
Si (control)	55.1 ± 0.4	35.0 ± 0.2	0	9.9 ± 0.6	0	0	0	3.5	0
DNA (control)	0	30.3 ± 1.4	8.8 ± 0.1	48.3 ± 1.9	3.5 ± 1.4	7.7 ± 0.7	1.5 ± 1.5	0.6	0.2
Si <500 bp PDNA	41.4 ± 4.8	30.1 ± 1.3	5.37 ± 2	22.9 ± 4.2	0	0.3	0	1.3	0.2
Si ~5–15 kbp PDNA	31.1 ± 4.5	29 ± 0.5	8.23 ± 1	29.2 ± 2	0	2.4 ± 1	0	1.0	0.3
Si >20 kbp PDNA	27.5 ± 0.6	28.7 ± 0.3	8.9 ± 0.2	32 ± 0.3	0	2.9 ± 0.2	0	0.9	0.3
AAMpp (control)	0	8.7 ± 0.1	16.7 ± 0.1	74.6 ± 0.2	0	0	0	0.1	0.2
AAMpp <500 bp PDNA	0	14 ± 0.1	15.6 ± 0.3	69 ± 0.1	1.2 ± 0.1	0.1	0	0.2	0.2
AAMpp ~5–15 kbp PDNA	0	14.7 ± 0.1	15.1 ± 0	68.3 ± 0.3	1.2 ± 0.1	0.6	0	0.2	0.2
AAMpp >20 kbp PDNA	0	15.7 ± 0.1	15.6 ± 0.3	65.8 ± 0.3	1.4 ± 0.1	1.5 ± 0.2	0	0.2	0.2
AAMpp <500 bp CDNA	0	15.4 ± 0.6	16.2 ± 0.2	66.6 ± 0.9	1.4 ± 0.1	0.4	0.1	0.2	0.2
AAMpp ~5–15 kbp CDNA	0	17.5 ± 0.6	15.2 ± 0.3	63.6 ± 1.3	1.7 ± 0.1	1.8 ± 0.5	0.1	0.3	0.2
AAMpp >20 kbp CDNA	0	16.8 ± 0.7	16 ± 0.4	64.7 ± 1.0	1.6 ± 0.1	0.8	0.1	0.3	0.2

observed and assigned to the hydrocarbon components (C—C/C—H) at 285.0 eV; and the other three peaks detected are due to the other forms of carbon contamination probably oxygen containing species. The C 1s spectrum of the control DNA surface [Fig. 2(b)] showed five components that are assigned to aliphatic hydrocarbon (C—C/C—H) at 285.0 eV; carbon bound to nitrogen (C—N) at 286.0 eV; carbon bound to oxygen (C—O) at 287.0 eV; the amide carbon (O=C—N) at 288.1 eV; and urea carbon [N—C(=O)—N] at 289.1 eV, which is quite similar to the literature[21–23] except it was possible to fit both C—O and C—N components due to the high resolution achievable with the analysis. In contrast, the C 1s spectra [Figs. 2(c)–2(e)] of the differently sized DNA (500 bp–20 kbp) physically adsorbed to the Si wafer surfaces showed only four components with the characteristic binding energies of 285.0 (C—C/C—H), 287.0 (C—N/C—O), 288.1 (O=C—N), and 289.2 [N—C(=O)—N] eV.

The Si wafer surface coated with AAMpp (Table I) demonstrated that the coating is thicker than the XPS sampling depth of 10 nm since only C, N, and O were detected, and the N/C ratio of 0.2 is in agreement with previous results for AAMpp coatings.[24] The detection of oxygen is due to free radical induced post-plasma oxidation of the AAMpp surface.[25] Physically absorbed and covalently immobilized DNA to the AAMpp surface showed further increments in O and the presence of DNA by detection of P from the sugar phosphate backbone of DNA. No significant changes in N/C and O/C ratios were observed since the AAMpp surface is also high in N, which masks the presence of immobilized DNA surfaces (Table I).

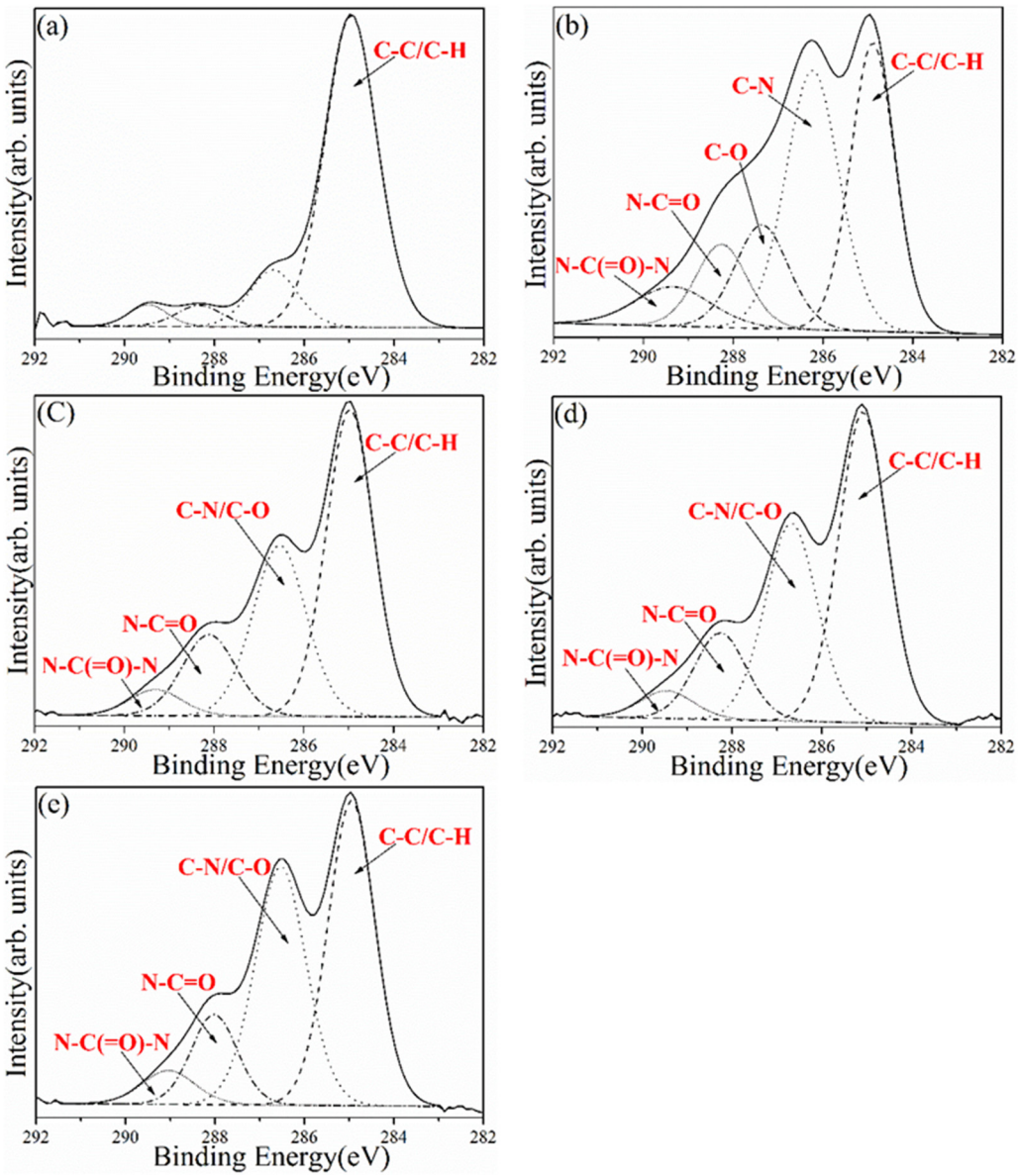

FIG. 2. High resolution C 1s XPS spectra of (a) Control Si surface, (b) Control DNA >20 kbp, (c) Si <500 bp PDNA, (d) Si ~5–15 kbp PDNA, and (e) Si>20 kbp PDNA.

There was no change observed in the N/C ratio; however, small amounts of P and NaCl were observed due to the attached DNA. Thereafter, these results also suggest that the plasma polymer coatings did not delaminate from the substrate when incubated overnight with the different DNA solutions and could thus be used also in bacterial culture experiments. The curve-fitted C 1s spectrum for a homogeneous film of AAMpp is shown in Fig. 3(a). Four component peaks were assigned to the hydrocarbon component (C—C/C—H) at 285.0 eV; carbon singly bonded with primary, secondary, or

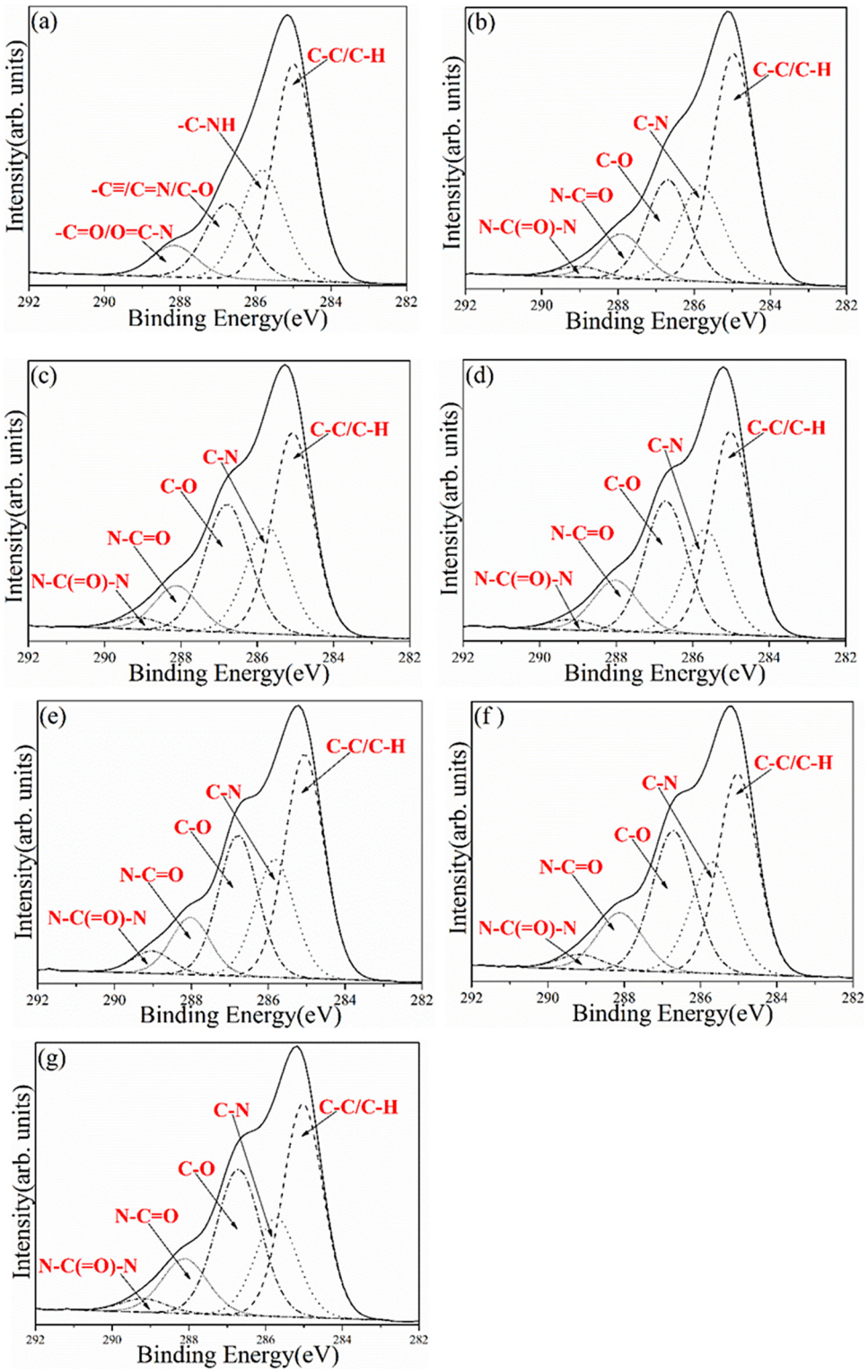

FIG. 3. XPS high resolution C 1s spectra of (a) Control AAMpp surface, (b) AAMpp <500 bp PDNA, (c) AAMpp ~5–15 kbp PDNA, (d) AAMpp >20 kbp PDNA, (e) AAMpp <500 bp CDNA, (f) AAMpp ~5–15 kbp CDNA, and (g) AAMpp >20 kbp CDNA.

TABLE II. Different sized physically adsorbed DNA film thickness and surface coverage on Si wafers based on assumptions 1 and 2 using N as the DNA element. Shown are mean values based on three analyses performed on each type of sample ($n = 3$).

	Assumption 1		Assumption 2	
Overnight immobilization of DNA	DNA film thickness (nm)	DNA surface coverage (ng/cm^2)	DNA film thickness (nm)	DNA surface coverage (ng/cm^2)
Si <500 bp PDNA	2.2	372	1.2	206
Si~5–15 kbp PDNA	4.5	763	2	357
Si >20 kbp PDNA	5.4	910	2.3	398

tertiary amine groups (—C—NH) at 285.6 eV; hydroxyls, ethers, imines, or nitriles (—C—O, —C=N, and —C≡N) at 286.6 eV; and aldehyde, ketones, or amides (—C=O and N—C=O) at 288.0 eV as supported by previous reports.[25,26]

The XPS data for DNA that is either physically adsorbed or covalently immobilized to AAMpp are also shown in Table I and demonstrate successful DNA attachment. As expected, both P and NaCl were detected and an increased concentration of O was observed. The high resolution C 1s spectra of physically adsorbed and covalently immobilized DNA of variable size are shown in Figs. 3(b)–3(g). The spectra can be fitted with five components of DNA, namely, C—C/C—H, C—N, C—O, N—C=O, and N—C(=O)—N with similar binding energies of, 285.0, 285.8, 286.7, 288.1, and 289.1 eV as shown above. There is no significant difference observed between physically adsorbed and covalently immobilized DNA on AAMpp surfaces. However, there is a slight increase in the C—O component as the size of the attached DNA increases. This is expected since from the structure of DNA a significant number of OH and C—O—C bonds appear in the base pairs thymine, cytosine, and guanine.

B. DNA film thickness determination

Table II shows the thickness and surface coverages of physically adsorbed DNA on the Si wafer surface based on the two assumptions made above. When the Sigma-Aldrich base pair content (%GC content: 41.2%; %AT content: 58.8%) is used, the thickness and surface coverage of adsorbed DNA is about twice as high as when equal contents of base pairs are used in the calculation.

Table III shows the thickness and surface coverage of physically and covalently immobilized DNA of different sizes on AAMpp surfaces based on the two assumptions described. The results show that for DNA attached to AAMpp surfaces the trend is reversed compared to the results for DNA adsorption to Si wafers. The calculated %P difference is not as variable as the calculated %N for the two assumptions made hence the variation in the values determined is not as great. In addition, the level of DNA is much lower for attachment to AAMpp compared to Si wafers; however, there is more covalently immobilized DNA than physically adsorbed DNA on the AAMpp surfaces. Overall, on Si wafer surfaces more DNA is attached compared to AAMpp, which could be viewed as a surprising result given the fact that AAMpp is positively charged and likely to attract more DNA if only electrostatic interactions are the driving force for DNA attachment. The comparative estimates of surface coverage derived from the XPS thickness measurements indicate that the arrangement of DNA on each surface is likely to be different. For the Si substrate, the coverages are estimated to be higher than on the AAMpp surface indicating that more molecules are immobilized and the packing density is likely to be higher for all sizes of DNA. For the AAMpp surface, there is likely to be very strong electrostatic attraction between the DNA and the positively charged amines of the AAMpp surface for the adsorbed DNA resulting in more molecules lying flat on the surface, since structural rearrangements are less likely.

TABLE III. Film thickness and surface coverages of differently sized DNA, either physically adsorbed or covalently immobilized to AAMpp surfaces, based on assumptions 1 and 2 when the bulk %P of DNA is used in the overlayer calculation. Shown are the mean values based on three analyses performed on each type of sample ($n = 3$).

	Assumption 1		Assumption 2	
Overnight immobilization of DNA	DNA film thickness (nm)	DNA surface coverage (ng/cm^2)	DNA film thickness (nm)	DNA surface coverage (ng/cm^2)
AAMpp <500 bp PDNA	0.86	146.3	1.14	193.8
AAMpp <500 bp CDNA	1.05	179	1.4	239.5
AAMpp ~5–15 kbp PDNA	0.87	147.9	1.16	197.2
AAMpp ~5–15 kbp CDNA	1.26	214.2	1.7	290
AAMpp >20 kbp PDNA	1.03	175.1	1.38	234.6
AAMpp >20 kbp CDNA	1.19	202.3	1.6	272

Similarly, for the covalent DNA, the reaction takes place between many of phosphate groups along the DNA backbone and the NH_2 groups on the AAMpp surface. Thus, this is likely to cause the DNA to also lie flat on the surface. Clearly, other physical forces influence how DNA interacts with surfaces. However, the important observation from the XPS results is that there is confirmation of the successful attachment of DNA on all surfaces and the estimates of the level could be related to the bacterial attachment results.

C. Effect of surface attached DNA on bacterial attachment and proliferation

The presence of DNA within bacterial culture media and intact biofilms has been shown not only to facilitate biofilm formation but also to stabilize the existing biofilms. However, since the initial stages of biofilm formation is the requirement that they attach to a solid substrate prior to proliferation into mature biofilms; a key question is whether the presence of DNA within the conditioning film enhances these processes. The other question is whether the stability of the DNA layer influences attachment and biofilm formation. In this respect, the aim was to test the hypothesis that a layer of DNA may significantly enhance attachment rates and if covalently immobilized (made more stable) then perhaps this may also have a positive influence on attachment and proliferation. The salmon sperm DNA surfaces prepared and characterized above were tested in attachment and proliferation assays using *P. aeruginosa* (ATCC-15692). For this study, differently sized DNAs (<500 bp, 5 kbp ~ 15 kbp, >20 kbp) were physically adsorbed onto Si wafer surfaces and also physically and covalently immobilized to AAMpp coated surfaces.

All these surfaces, including control Si and AAMpp surface, were exposed to bacteria cultures for 1- and 4-h static assays in MBH media, followed by subsequent formaldehyde treatment for fixing bacteria on the surface and Live/Dead staining for epi-fluorescence imaging. Due to the formaldehyde treatment, all attached bacteria had died and stained red in color. Representative Live/Dead stained epi-fluorescence microscopy images of the 1-h attached bacteria on DNA functionalized surfaces are shown in Figs. 4(a)–4(k). The control Si surface [Fig. 4(a)] showed a high coverage of bacteria with some clusters of bacteria also being observed. On the other hand, the AAMpp coated surface [Fig. 4(e)] showed almost complete coverage of bacteria compared to the Si surface. These observations are also seen in the SEM images of attached bacteria on control Si wafers [Fig. 6(a)] and the AAMpp coating [Fig. 6(e)]. The possible explanation for these phenomena is that the amine rich AAMpp substrate contains a positive charge and it is appealing to the bacteria. Since the extracellular polysaccharide (EPS) layer on the *P. aeruginosa* cell surfaces is negatively charged which develops a strong electrostatic attraction.[27–30]

Interestingly, the 1-h bacterial attachment to DNA coated surfaces showed quite contrasting results. Small to large sized physically adsorbed DNA on Si wafer surfaces [Figs. 4(b)–4(d)] and physically adsorbed [Figs. 4(f)–4(h)] and covalently [Figs. 4(i)–4(k)] attached DNA on AAMpp

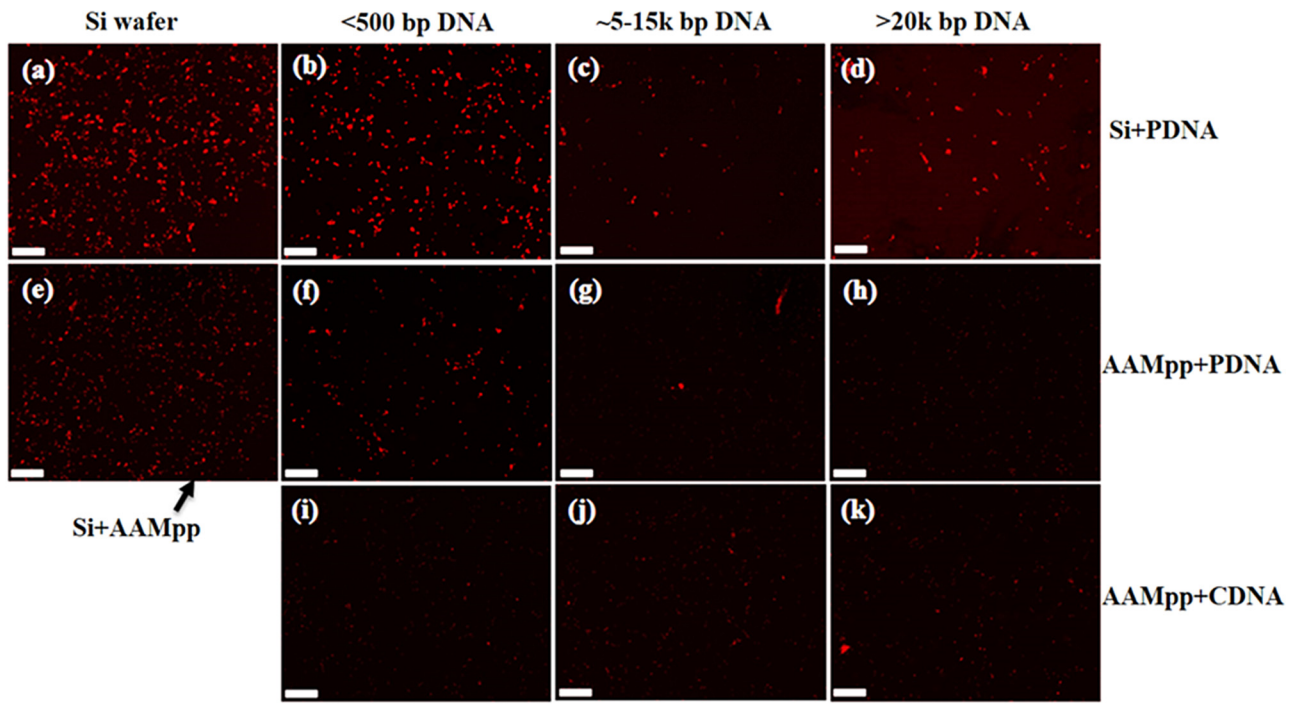

FIG. 4. Epi-fluorescence images of Live/Dead stained *P. aeruginosa* after 1 h attachment to (a) Si, (b) Si <500 bp PDNA, (c) Si ~5–15 kbp PDNA, (d) Si >20 kbp PDNA, (e) AAMpp, (f) AAMpp <500 bp PDNA, (g) AAMpp ~5–15 kbp PDNA, (h) AAMpp >20 kbp PDNA, (i) AAMpp <500 bp CDNA, (j) AAMpp ~5–15 kbp CDNA, and (k) AAMpp >20 kbp CDNA. All scale bars: 50 μm.

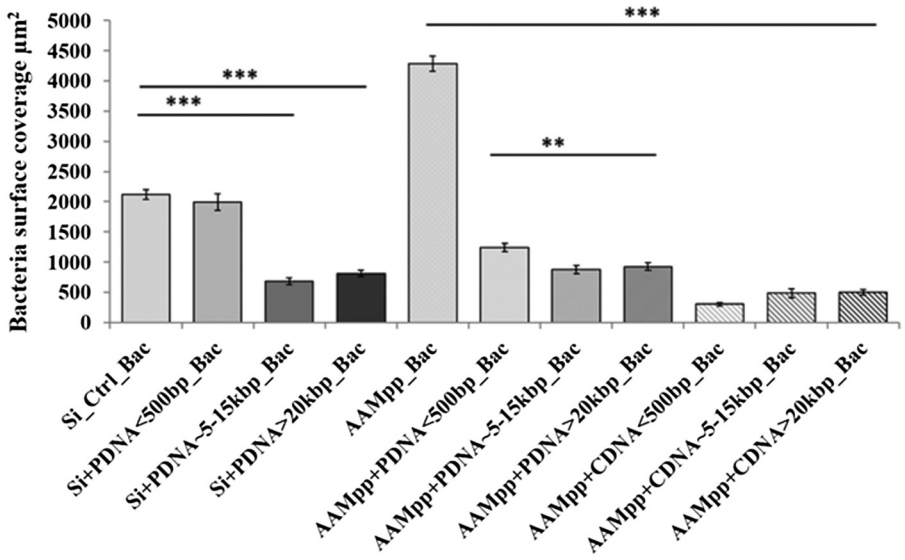

FIG. 5. Comparison of *P. aeruginosa* surface coverage after 1 h attachment on different types of surfaces including Si wafer control, AAMpp control, and differently sized DNA attached on Si and AAMpp. $***p < 0.001$, $**p < 0.01$. Data shown: mean ± standard error of the mean ($n = 10$).

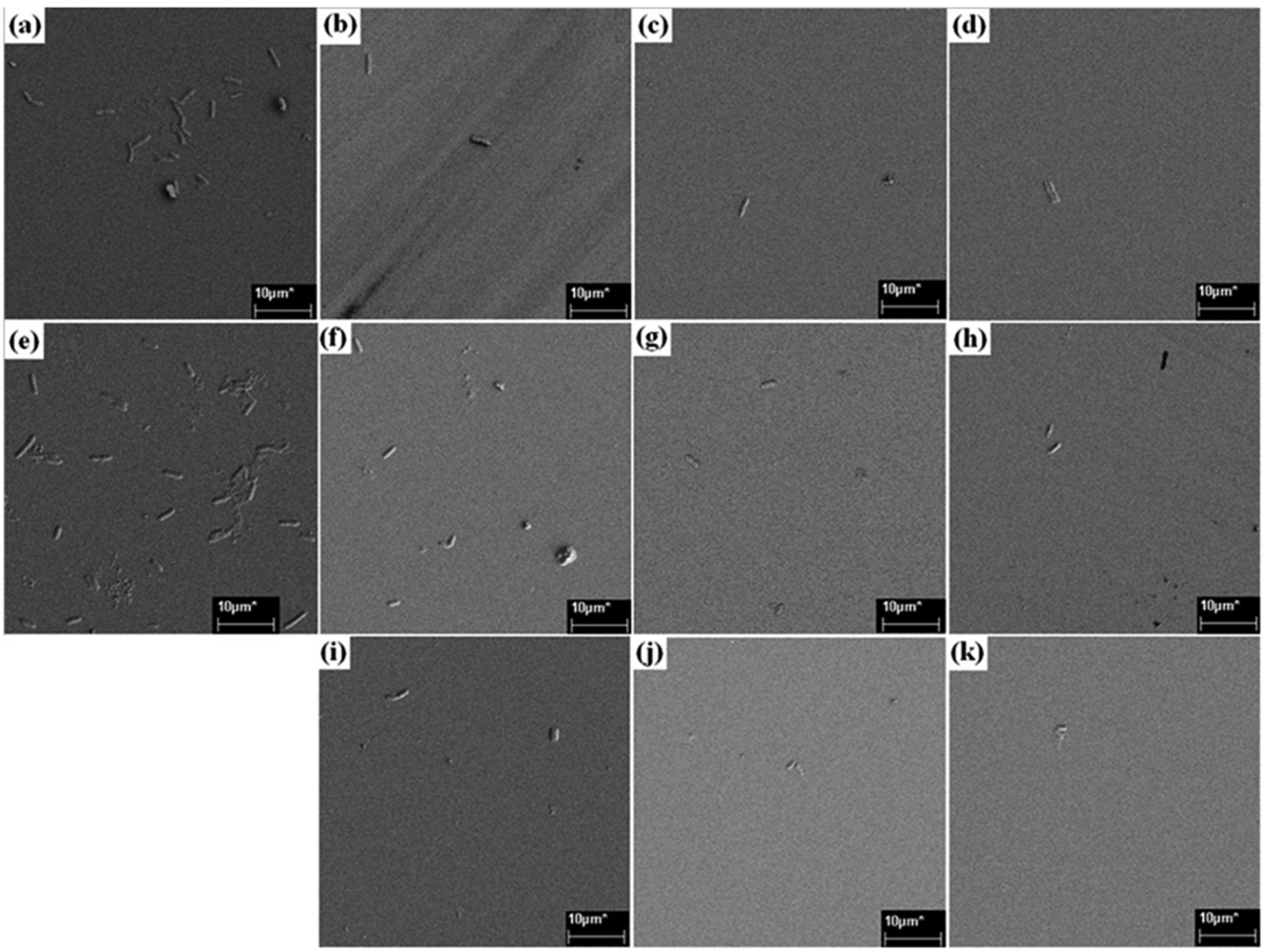

FIG. 6. Low magnification SEM images of 1 h *P. aeruginosa* attachment onto (a) Si, (b) Si <500 bp PDNA, (c) Si ~5–15 kbp PDNA, (d) Si >20 kbp PDNA, (e) AAMpp, (f) AAMpp <500 bp PDNA, (g) AAMpp ~5–15 kbp PDNA, (h) AAMpp >20 kbp PDNA, (i) AAMpp <500 bp CDNA, (j) AAMpp ~5–15 kbp CDNA, and (k) AAMpp >20 kbp CDNA. All scale bars: 10 μm.

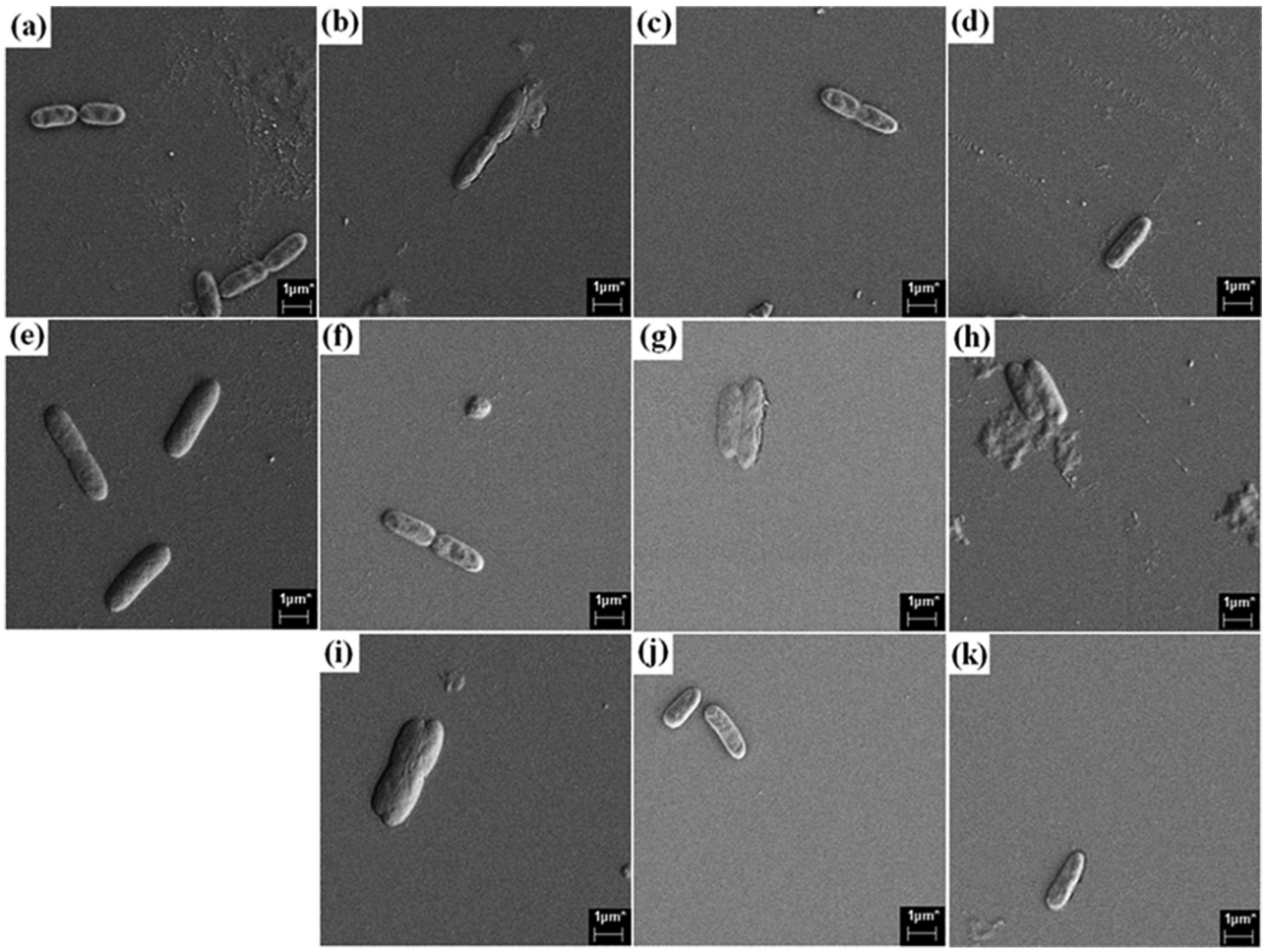

FIG. 7. High magnification SEM images of 1 h *P. aeruginosa* attachment onto (a) Si, (b) Si <500 bp PDNA, (c) Si ~5–15 kbp PDNA, (d) Si >20 kbp PDNA, (e) AAMpp, (f) AAMpp <500 bp PDNA, (g) AAMpp ~5–15 kbp PDNA, (h) AAMpp >20 kbp PDNA, (i) AAMpp <500 bp CDNA, (j) AAMpp ~5–15 kbp CDNA, and (k) AAMpp >20 kbp CDNA. All scale bars: 1 μm.

surface showed negligible amounts of bacteria attachment compared to the Si and AAMpp [Figs. 4(a) and 4(e)] control surfaces.

Quantitative analysis of the surface coverage of *P. aeruginosa* on the differently sized DNA attached surfaces after 1 h is shown in Fig. 5, confirming the results of the comparative images in Fig. 4. There is no difference observed in the levels of bacterial attachment on the control Si and the small size (<500 bp) DNA attached Si surface after 1 h bacteria culture. However, significant differences in bacterial attachment are observed between the control Si surface and medium (~5–15 kbp) and large (>200 kbp) sized DNA functionalized surfaces, i.e., $p^{xxx} < 0.001$. Thereafter, there is no significant difference observed in bacterial attachment on the medium and large sized DNA attached surfaces. In contrast, when the AAMpp coated control is compared with all six physically adsorbed and covalently immobilized DNA surfaces; the quantitative data show huge reductions in bacterial attachment, i.e., $p^{xxx} < 0.001$. As we showed previously, bacteria like to attach more on the AAMpp surface compared to control glass, which is also confirmed statistically in Fig. 5.

SEM analysis was performed on the same samples used to generate the epi-fluorescence images, and the resultant images are shown in Fig. 6 (low magnification) and Fig. 7 (high magnification). The micrographs further support the results obtained through epi-fluorescence images and the quantitative analysis of the resultant images. Compared to the control (Si and AAMpp) surfaces, all DNA coated surfaces showed much lower amounts of bacterial attachment.

In order to study longer term attachment, all surfaces were exposed to *P. aeruginosa* culture for 4 h. In contrast to the 1-h attachment results, both Si wafer [Fig. 8(a)] and AAMpp [Fig. 8(e)] control surfaces showed similar and almost confluent surface coverages of bacteria. The most likely reason for this is the positive surface charge of AAMpp surface being more attractive to the EPS rich *P. aeruginosa* surfaces at short culture times, and when the culture time increases to 4 h, more bacteria are found to attach to both controls. Similar observations are also seen in the SEM images of bacteria on Si [Fig. 10(a)] and on the AAMpp [Fig. 10(e)] controls. The Si surfaces with physically adsorbed DNA [Figs. 8(b)–8(d)] and the AAMpp with physically adsorbed [Figs. 8(f)–8(h)] and covalently immobilized

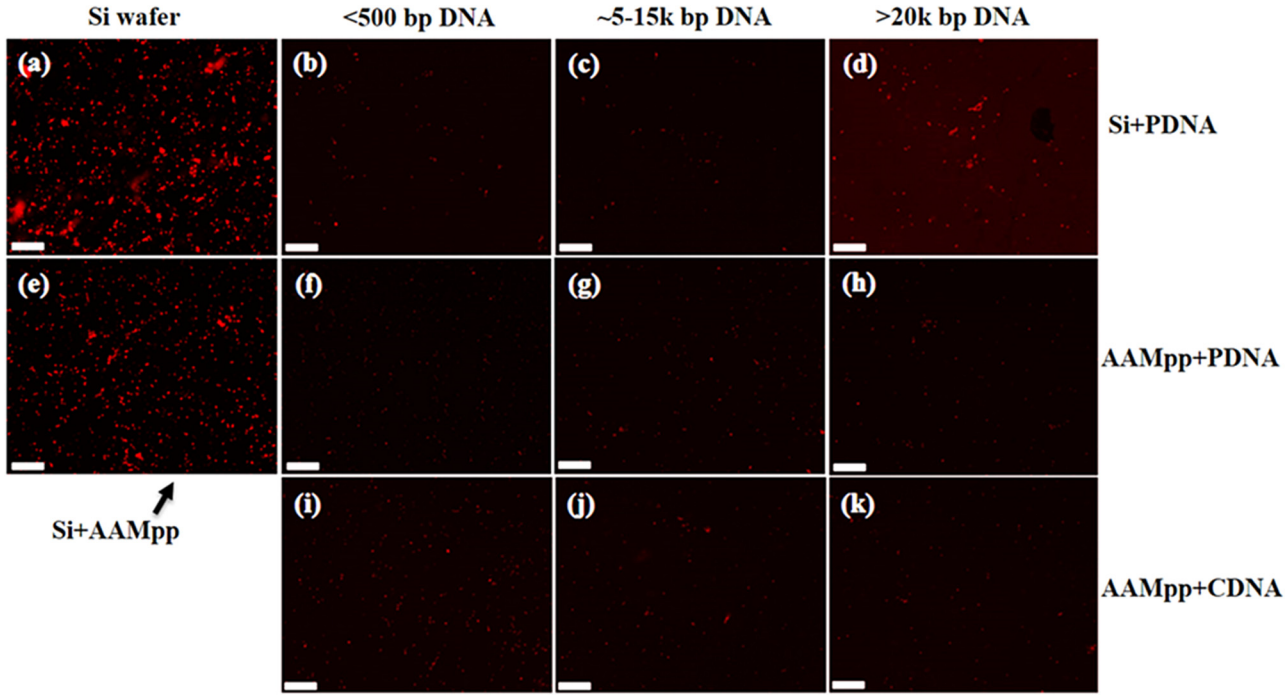

FIG. 8. Epi-fluorescence images of Live/Dead stained *P. aeruginosa* after 4 h attachment on (a) Si, (b) Si <500 bp PDNA, (c) Si ~5–15 kbp PDNA, (d) Si >20 kbp PDNA, (e) AAMpp, (f) AAMpp <500 bp PDNA, (g) AAMpp ~5–15 kbp PDNA, (h) AAMpp >20 kbp PDNA, (i) AAMpp <500 bp CDNA, (j) AAMpp ~5–15 kbp CDNA, and (k) AAMpp >20 kbp CDNA. All scale bars: 50 μm.

DNA [Figs. 8(i)–8(k)] showed similar results to the 1-h culture in that substantially fewer bacterial attachment occurs on all types of DNA coated surfaces compared to the Si and AAMpp [Figs. 8(a) and 8(e)] control surfaces.

Finally, quantitative analysis of the surface coverage of *P. aeruginosa* after 4 h of culture on the differently sized DNA coated Si and AAMpp surfaces (Fig. 9) confirms the results of the visual images in Fig. 8. There is a significant difference observed in the levels of bacterial attachment on the control Si and all differently sized DNA attached Si and AAMpp surfaces, i.e., $p^{xxx} < 0.001$. There is also no significant difference in bacterial attachment between the differently sized DNA coated Si surfaces. Thus, up to 4 h culture, the DNA shows a significant repulsion against *P. aeruginosa* biofilm formation. There are, however, significant differences in bacterial attachment between the small size (<500 bp) and large size (>20 kbp) DNA coatings on the AAMpp surface, i.e., $*p < 0.05$, $p^{xx} < 0.01$, for both physically adsorbed and covalently immobilized DNA.

On the AAMpp surfaces, both physically and covalently immobilized DNA showed significant decreases in bacterial attachment. However, increasing the size of the pre-adsorbed DNA (both physically and covalently) on the AAMpp surface resulted in more reductions in bacterial attachment. Low and high resolution SEM images shown in Fig. 10 (low magnification) and Fig. 11 (high magnification) also confirm the results obtained through epi-fluorescence images (Fig. 8) and the quantitative analysis (Fig. 9) of the resultant images.

In both the 1- and 4-h static *P. aeruginosa* culture, the results proved very surprising since the differently sized DNA coated surfaces, either physically adsorbed or covalently immobilized, showed high reductions in the level of bacterial attachment. Therefore, although the literature reports show that eDNA is a helpful component in enhancing initial bacterial attachment and in the subsequent stability of a mature biofilm one needs to consider that the DNA molecules may not enhance bacterial attachment through interactions with DNA adsorbed to surfaces. Most likely the DNA enhances bacterial activity and biofilm forming capabilities in the planktonic state. XPS results confirmed the successful grafting of DNA under both physical and covalent attachment conditions. Longer (>20 kbp) DNA molecules showed good coverage and thickness on both types of surfaces. Clearly, the salmon sperm DNA coatings used here have some antifouling properties by not allowing bacteria to make proper initial contact on these abiotic surfaces. Harmsen *et al.*[5] studied the role of eDNA in *Listeria monocytogenes* biofilm formation and found that the size of eDNA is a very important factor of initial bacterial attachment. In their study, they showed that when adding low molecular weight eDNA < 500 bp to eDNA-free cells in culture adhesion was eliminated, while high-molecular weight eDNA combined with some other supernatant components support bacterial adhesion. Also, we have recently shown that addition of purified *P. aeruginosa* DNA did not complement the biofilm forming capabilities of mutants unable to release their own eDNA through explosive cell lysis, and we proposed that other components released through lysis are required to initiate the development of biofilms.[31]

In another study, Berne *et al.*[32] demonstrated that with *Caulobacter crescentus* (*C. crescentus*) eDNA inhibits its

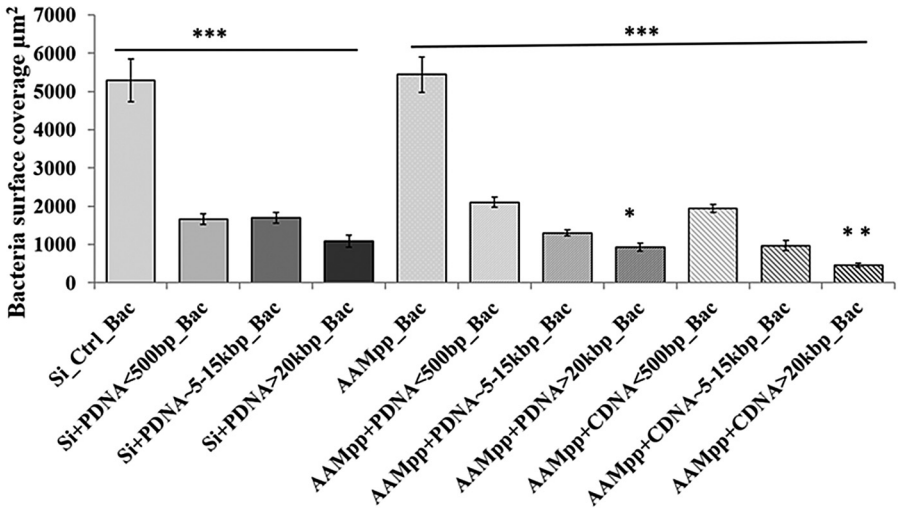

FIG. 9. Comparison of 4 h *P. aeruginosa* surface coverages on, Si, AAMpp controls, and differently sized DNA coated Si, AAMpp. $***p < 0.001$, $**p < 0.01$, $*p < 0.05$. Data shown: mean ± standard error of the mean ($n = 10$).

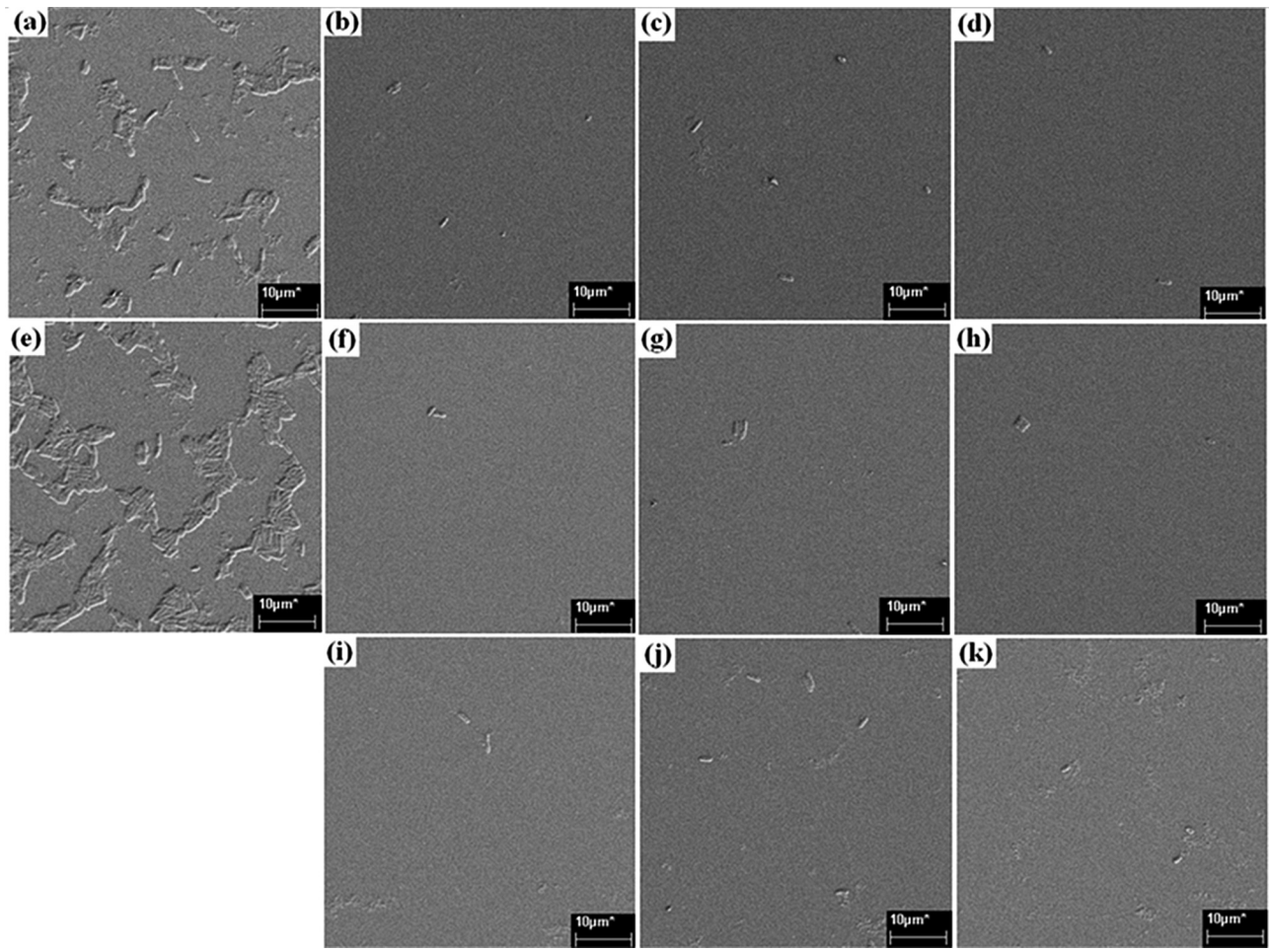

FIG. 10. Low resolution SEM images of 4 h *P. aeruginosa* attachment on flat: (a) Si, (b) Si <500 bp PDNA, (c) Si ~5–15 kbp PDNA, (d) Si >20 kbp PDNA, (e) AAMpp, (f) AAMpp <500 bp PDNA, (g) AAMpp ~5–15 kbp PDNA, (h) AAMpp >20 kbp PDNA, (i) AAMpp <500 bp CDNA, (j) AAMpp ~5–15 kbp CDNA, and (k) AAMpp >20 kbp CDNA. All scale bars: 10 μm.

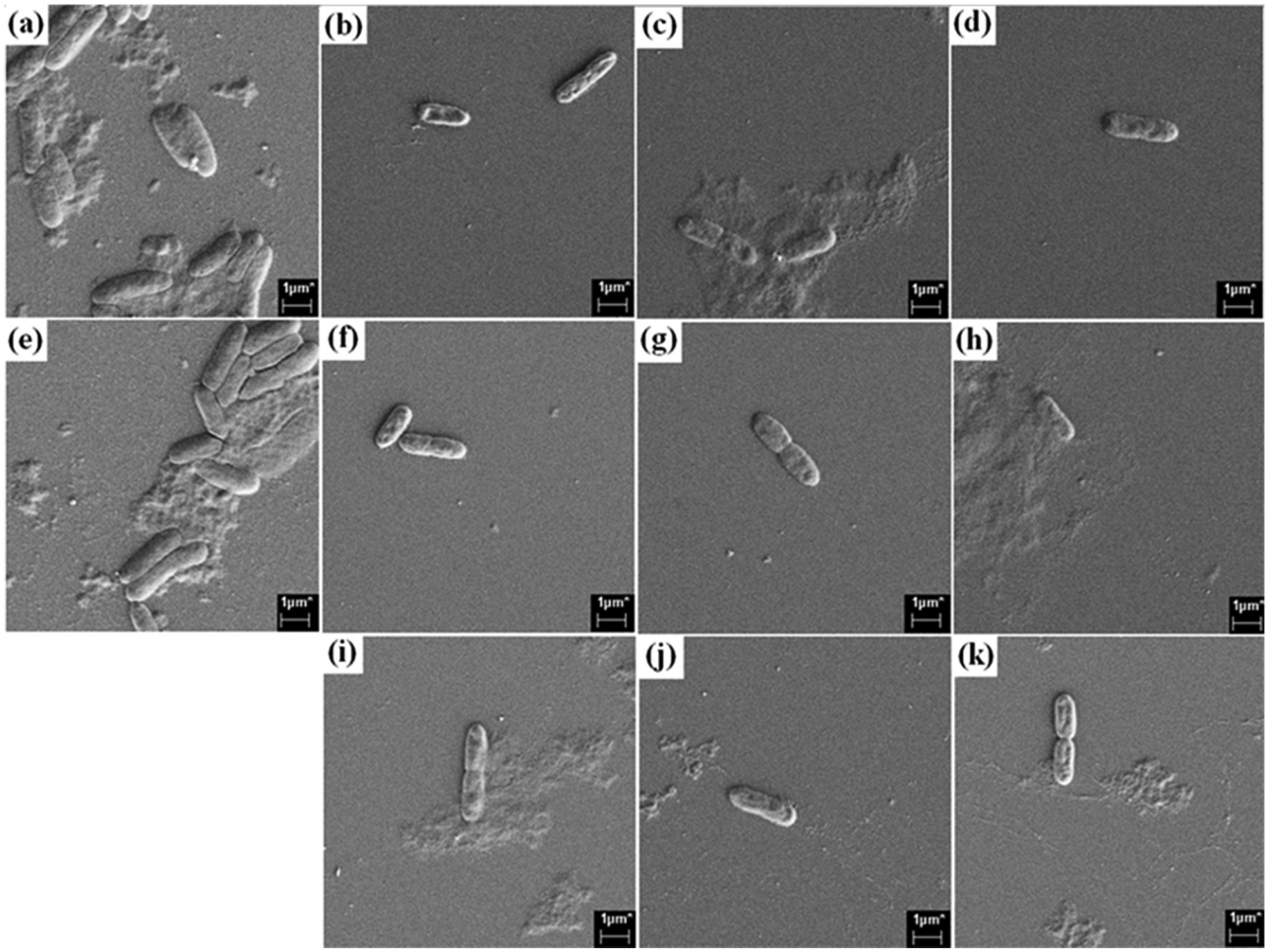

FIG. 11. High resolution SEM images of 4 h *P. aeruginosa* attachment on flat: (a) Si, (b) Si <500 bp PDNA, (c) Si ~5–15 kbp PDNA, (d) Si >20 kbp PDNA, (e) AAMpp, (f) AAMpp <500 bp PDNA, (g) AAMpp ~5–15 kbp PDNA, (h) AAMpp >20 kbp PDNA, (i) AAMpp <500 bp CDNA, (j) AAMpp ~5–15 kbp CDNA, and (k) AAMpp >20 kbp CDNA. All scale bars: 1 μm.

own motility to settle into a biofilm. The reason for this is eDNA binds holdfast (adhesive polar polysaccharide synthesized by *C. crescentus* for surface attachment) to bacterial cells, a structure of cells which is essential in permanent attachment to surfaces. Furthermore, Wang *et al.*[33] found significantly contrasting results with more biofilm formation occurring after DNase I treatment with *Salmonella enterica, Serovar typhimurium* and *Salmonella enterica Serovar*, indicating that bacteria were more likely to attach to abiotic surfaces in the presence of DNase I and are able to form large compact biofilms. Additionally, when they added exogenous eDNA to the bacterial culture, an observable decrease in biofilm formation was observed. All these studies showed that eDNA can reduce bacterial attachment on surfaces, but in all cases eDNA was provided as an external component to the bacterial culture, while in this study we have pre-adsorbed/immobilized different sizes of DNA directly on the surface.

To the best of our knowledge, this is the first study reporting the antifouling effect of surface attached DNA on *P. aeruginosa* attachment. Dickson and Koohmaraie[34] demonstrated that there is a linear relationship between bacterial cell surface charge and their attachment to surfaces. In these studies, electrostatic repulsion could be the reason of the antifouling behavior of the surface attached DNA, because DNA contains a net negative charge due to the presence of the phosphate backbone and bacterial cell surface also possesses a net negative charge. However, the open question remains: does DNA added to growth media actually see the surface? Given the potential high concentrations present in media, it may be possible that on occasions some DNA reaches the surface, adding speculation that the contrasting reports between different labs is a result of not the composition of the growth media but the composition of the conditioning films that form, of which DNA is a potential adsorbate. Furthermore, bacterial viability and initial attachment depend on lots of factors including the length of DNA, type of DNA, and also bacterial strain. Thus, the approaches presented here could be an essential tool in bacterial attachment studies on abiotic surfaces. However, these results are preliminary and further experiments are needed including longer culture times both in static and in flowing experiments including the use of different bacterial strains to ascertain whether the promising initial findings are universal.

IV. CONCLUSIONS

In conclusion, different sizes of salmon sperm DNA were successfully physically adsorbed and covalently immobilized on Si wafer and AAMpp surfaces to different extents as shown from the XPS analysis. These DNA coated surfaces were then exposed to *P. aeruginosa* suspensions in static cultures for 1 and 4 h. It was demonstrated that there was a size dependent relationship in the ability to repel *P. aeruginosa* attachment at both culture times and that for some sizes of DNA covalent attachment showed small but more significant reductions in attachment compared to physical adsorption. These preliminary results establish a new platform for bacterial attachment studies on DNA coated surfaces. We believe that for short term prevention of bacterial attachment, DNA coated surfaces or surfaces that attract DNA may be a useful approach. In future work, studies based on DNA patterns may further reduce or slow down initial attachment of bacteria on surfaces. Further detailed studies are needed to understand the exact phenomena of antifouling behavior of surfaces precoated with DNA.

ACKNOWLEDGMENTS

The Australian Research Council (ARC) is acknowledged for funding a Ph.D. scholarship for HP through a Discovery Project (No. DP120103405) and for funding P.-Y.W. through a Discovery Early Career Researcher Award (No. ARC-DECRA) (No. DE150101755). Taipei Medical University and Ministry of Science and Technology are also acknowledged for providing funding support for P.-Y.W. (Nos. TMU105-AE1-B13 and 105-2314-B-038-088-MY2). This work was supported in part at both the Biointerface Engineering Hub at Swinburne and the Melbourne Centre for Nanofabrication as part of the Victorian Node of the Australian National Fabrication Facility, a company established under the National Collaborative Research Infrastructure Strategy to provide nano- and microfabrication facilities for Australia's researchers.

[1]A. Dell'Anno and R. Danovaro, Science **309**, 2179 (2005).
[2]J. Niemeyer and F. Gessler, J. Plant Nutr. Soil Sci. **165**, 121 (2002).
[3]D. Vorkapic, K. Pressler, and S. Schild, Curr. Genet. **62**, 71 (2016).
[4]M. Allesen-Holm, K. B. Barken, L. Yang, M. Klausen, J. S. Webb, S. Kjelleberg, S. Molin, M. Givskov, and T. A. Tolker-Nielsen, Mol. Microbiol. **59**, 1114 (2006).
[5]M. Harmsen, M. Lappann, S. Knøchel, and S. Molin, Appl. Environ. Microbiol. **76**, 2271 (2010).
[6]C. B. Whitchurch, T. Tolker-Nielsen, P. C. Ragas, and J. S. Mattick, Science **295**, 1487 (2002).
[7]M. S. Conover, M. Mishra, and R. Deora, PLoS One **6**, e16861 (2011).
[8]T. Das, P. K. Sharma, B. P. Krom, H. C. van der Mei, and H. J. Busscher, Langmuir **27**, 10113 (2011).
[9]P. K. Chu, J. Chen, L. Wang, and N. Huang, Mater. Sci. Eng. R Rep. **36**, 143 (2002).
[10]C.-Y. Lee, G. M. Harbers, D. W. Grainger, L. J. Gamble, and D. G. Castner, J. Am. Chem. Soc. **129**, 9429 (2007).
[11]H. Cai, X. Cao, Y. Jiang, P. He, and Y. Fang, Anal. Bioanal. Chem. **375**, 287 (2003).
[12]H. J. Griesser, Vacuum **39**, 485 (1989).
[13]M. R. Vilar, A. M. Botelho do Rego, A. M. Ferraria, Y. Jugnet, C. Nogues, D. Peled, and R. Naaman, J. Phys. Chem. B **112**, 6957 (2008).
[14]S. Tanuma, C. J. Powell, and D. R. Penn, Surf. Interface Anal. **21**, 165 (1994).
[15]F. Gautier, H. Bunemann, and L. Grotjahn, Eur. J. Biochem. **80**, 175 (1977).
[16]H. Votavova and J. Šponar, Nucleic Acids Res. **2**, 431 (1975).
[17]J. Filipski, J.-P. Thiery, and G. Bernardi, J. Mol. Biol. **80**, 177 (1973).
[18]C. J. May, H. E. Canavan, and D. G. Castner, Anal. Chem. **76**, 1114 (2004).
[19]D. Y. Petrovykh, H. Kimura-Suda, L. J. Whitman, and M. J. Tarlov, J. Am. Chem. Soc. **125**, 5219 (2003).
[20]B. Saoudi, N. Jammul, M. M. Chehimi, A.-S. Jaubert, C. Arkam, and M. Delamar, J. Spectrosc. **18**, 519 (2004).
[21]C.-Y. Lee, P. Gong, G. M. Harbers, D. W. Grainger, D. G. Castner, and L. J. Gamble, Anal. Chem. **78**, 3316 (2006).
[22]S. Ptasińska, A. Stypczyńska, T. Nixon, N. J. Mason, D. V. Klyachko, and L. Sanche, J. Chem. Phys. **129**, 08B604 (2008).
[23]D. Y. Petrovykh, H. Kimura-Suda, M. J. Tarlov, and L. J. Whitman, Langmuir **20**, 429 (2004).
[24]S. W. Myung and H. S. Choi, Korean J. Chem. Eng. **23**, 505 (2006).
[25]B. Finke, H. Rebl, F. Hempel, J. Schäfer, K. Liefeith, K.-D. Weltmann, and J. B. Nebe, Langmuir **30**, 13914 (2014).
[26]F. Fally, C. Doneux, J. Riga, and J. Verbist, J. Appl. Polym. Sci. **56**, 597 (1995).
[27]H. Pingle, P.-Y. Wang, H. Thissen, S. L. McArthur, and P. Kingshott, Biointerphases **10**, 04A309 (2015).
[28]P. Hamerli, T. Weigel, T. Groth, and D. Paul, Biomaterials **24**, 3989 (2003).
[29]T. Jacobs, R. Morent, N. De Geyter, P. Dubruel, and C. Leys, Plasma Chem. Plasma Process. **32**, 1039 (2012).
[30]R. Förch *et al.*, Chem. Vap. Deposition **13**, 280 (2007).
[31]L. Turnbull *et al.*, Nat. Commun. **7**, 11220 (2016).
[32]C. Berne, D. T. Kysela, and Y. V. Brun, Mol. Microbiol. **77**, 815 (2010).
[33]H. Wang, Y. Huang, S. Wu, Y. Li, Y. Ye, Y. Zheng, and R. Huang, Curr. Microbiol. **68**, 262 (2014).
[34]J. S. Dickson and M. Koohmaraie, Appl. Environ. Microbiol. **55**, 832 (1989), available at https://aem.asm.org/content/55/4/832.